



Published in final edited form as:

*Lasers Surg Med.* 2008 October ; 40(8): 535–542. doi:10.1002/lsm.20670.

## Disruption of the Blood–Brain Barrier Following ALA-Mediated Photodynamic Therapy

Henry Hirschberg, MD, PhD<sup>1,2,\*</sup>, Francisco A. Uzal, DVM, PhD<sup>3</sup>, David Chighvinadze, MS<sup>2</sup>, Michelle J. Zhang, BS<sup>2</sup>, Qian Peng, PhD<sup>4</sup>, and Steen J. Madsen, PhD<sup>2</sup>

<sup>1</sup>Beckman Laser Institute, University of California, Irvine, California 92612

<sup>2</sup>Department of Health Physics, University of Nevada, Las Vegas, Nevada 89154

<sup>3</sup>School of Veterinary Medicine, University of California, Davis, San Bernardino, California 92408

<sup>4</sup>Department of Pathology, The Norwegian Radium Hospital, Oslo, Norway

### Abstract

**Background and Objective**—Photodynamic therapy (PDT) is a local antineoplastic treatment with the potential for tumor cell specificity. PDT using either hematoporphyrin derivatives or 5-aminolevulinic acid (ALA) has been reported to induce brain edema indicating disruption of the blood–brain barrier (BBB). We have evaluated the ability of ALA-mediated PDT to open the BBB in rats. This will permit access of chemotherapeutic agents to brain tumor cells remaining in the resection cavity wall, but limit their penetration into normal brain remote from the site of illumination.

**Study Design/Materials and Methods**—ALA-PDT was performed on non-tumor bearing inbred Fischer rats at increasing fluence levels. Contrast T<sub>1</sub>-weighted high field (3 T) magnetic resonance imaging (MRI) scans were used to monitor the degree of BBB disruption which could be inferred from the intensity and volume of the contrast agent visualized.

**Results**—PDT at increasing fluence levels between 9 and 26 J demonstrated an increasing contrast flow rate. A similar increased contrast volume was observed with increasing fluence rates. The BBB was found to be disrupted 2 hours following PDT and 80–100% restored 72 hours later at the lowest fluence level. No effect on the BBB was observed if 26 J of light was given in the absence of ALA.

**Conclusion**—ALA-PDT was highly effective in opening the BBB in a localized region of the brain. The degradation of the BBB was temporary in nature at fluence levels of 9 J, opening rapidly following treatment and significantly restored during the next 72 hours. No signs of tissue damage were seen on histological sections at this fluence level. However, higher fluences did demonstrate permanent tissue changes localized in the immediate vicinity of the light source.

### Keywords

brain edema; fischer rat; fluence; fluence rate; magnetic resonance imaging; malignant glioma

### Introduction

Despite improvements in currently employed treatment methods for malignant gliomas including surgical tumor resection, radio- and/or chemotherapy, patient prognosis remains poor. Malignant cells of these high-grade gliomas exhibit migratory behavior, possibly owing

\*Correspondence to: Henry Hirschberg, MD, PhD, Beckman Laser Institute, 1002 Health Sciences Rd., Irvine, CA 92612. E-mail: hhirschb@uci.edu.

to their developmental character within the CNS and, as a consequence, patients relapse in almost all cases with recurrent tumor growth within a 2–3 cm margin of the surgical resection cavity [1]. This appears to be the rule even in cases where post-operative MRI shows no residual tumor. The CNS is protected from circulating toxins by the relatively impenetrable BBB. The BBB prevents passage of ionized water-soluble molecules with molecular weight greater than 180 Da as well as large lipophilic compounds [2]. Consequently, the BBB limits the delivery of potentially effective diagnostic or therapeutic agents and this is probably the reason that chemotherapy has only contributed marginal patient benefit [3]. Although the BBB may be partially disrupted in gliomas, as shown experimentally by the uptake of horseradish peroxidase [4], clinically by improved visualization of the tumor by contrast-enhanced magnetic resonance imaging (MRI), or fluorescence measurements following the injection of photosensitizers [5], the brain adjacent to tumor (BAT) is characterized by relatively intact barriers. Therefore, even if the main tumor mass has a permeable vascular endothelium, the peripheral BAT region, which contains infiltrative tumor cells, has decreased permeability to anti-tumor agents. This poses a significant therapeutic challenge since these infiltrative tumor cells are protected by a patent BBB. For a drug delivery system to be successful at preventing tumor recurrence, transient and localized targeting of BBB disruption in the wall of the resection cavity following surgical removal of the bulk tumor, is necessary.

PDT is a local antineoplastic treatment with the potential for tumor cell specificity. The treatment involves the administration of a tumor-localizing photosensitizing agent followed by photo activation within the malignant tissue [6]. Several studies have shown that PDT may prove useful in prolonging survival and/or improving the quality-of-life in glioma patients [7–9]. PDT has several features that makes it a potentially effective adjuvant therapy for the treatment of brain tumors: (1) PDT is a local form of treatment in which the treated volume is limited by high attenuation of light in brain tissues and, (2) repeated application of PDT is an option due to low long-term morbidity.

The aim of PDT is to eliminate the nests of tumor cells remaining in the margins of the resection cavity following surgical removal of the bulk tumor while causing minimum damage to the surrounding brain tissue. In particular, PDT delivered in repetitive form has been shown in both experimental and clinical studies to have clear advantages over single treatments [9–11].

PDT using either hematoporphyrin derivatives or ALA has been reported to induce brain edema [12–15]. The edema region surrounding the site of light treatment suggests a local degradation of the BBB. PDT therefore appears to have a twofold effect; a direct antineoplastic effect on the remaining tumor cells as well as an effect that results in localized opening of the BBB allowing chemotherapeutic agents to penetrate into the BAT region.

The present study investigates changes in the BBB following ALA-PDT in normal rodent brain. The use of MRI allows for a more detailed study of the dynamics of blood–brain barrier degradation following PDT compared to that which can be obtained with more conventional methods. MRI scans at 3 T following intra-peritoneal gadolinium (Gd) contrast administration allowed for a highly detailed spatial and temporal analysis of the BBB opening.

## Materials and Methods

### Experimental Animals

Inbred male Fischer 344 rats (Simonsen Laboratories, Inc., Gilroy, CA) weighing at least 300 g were caged in Macrolon III cages. The animal holding rooms were maintained at constant temperature and humidity on a 12-hour light and dark schedule at an air exchange rate of 18 changes per hour. Animal care and protocol were in accordance with institutional guidelines. For the surgical procedures, the rats were anaesthetized with pentobarbital (25 mg/kg i.p.).

Buprenorphin (0.08 mg/kg s.c.) was used as a post-operative analgesic. The animals received a total of seven doses administered at 12-hour intervals. All animals were euthanized with Pentobarbital (100 mg/kg i.p.) at the first signs of distress.

### **PDT Treatment Protocol**

Four to five hours following ALA administration (125 mg/kg i.p), the animals were anaesthetized and fixed in a stereotactic frame. A skin incision was opened and a 1 mm burr hole was made. A 400 µm bare flat-end quartz fiber with numerical aperture 0.22 was introduced stereotactically directly into the brain to a depth of 5 mm below the dura. Light from a 632 nm diode laser was delivered interstitially to various fluence levels at different fluence rates over a time interval ranging from 10 to 90 minutes. After treatment, the fiber was withdrawn and closure was performed with bone wax and sutures.

### **Magnetic Resonance Imaging**

Fischer rats were imaged in a 3.0 T human MR scanner (Achieva X-series, Philips Medical Systems, Bothell, WA). At various times following treatment, animals were anesthetized and subjected first to T2-weighted (TR = 3,560 milliseconds; TE = 80 milliseconds) fast spin echo pulse sequences followed by T1-weighted fast spin echo pulse sequences (TR = 495 milliseconds; TE = 10 milliseconds, slice thickness = 1.0 mm) obtained before and after a subcutaneous injection of Gd contrast (1.0 ml of 0.5 mmol/ml Magnevist; Berlex Laboratories, Wayne, NJ). In the post-contrast studies, images were acquired over a time interval of 10–60 minutes following Gd administration. In all cases, animals were imaged using a receiver coil designed for scanning the human shoulder.

The estimation of Gd concentration was performed as follows. Four calibration tubes with known Gd concentrations in saline were scanned and the intensities analyzed (Fig. 1a). It was assumed that the relationship between the Gd concentration and the signal intensity in white and gray matter were similar to that of the calibration tubes, and therefore the calibration curve derived from these measurements could be extrapolated to brain tissue (Fig. 1b).

### **Histological Preparation**

Animals were sacrificed 14 days following PDT treatment and their brains extracted. The brains were sectioned along the fiber injection track and fixed by immersion in 10% buffered (pH 7.2) formalin prior to paraffin embedding. Four micrometer thick coronal sections were obtained from the original cut surface representing the position of the fiber track and thereafter at 1, 2, and 3 mm depths. The sections were stained with hematoxylin and eosin (H&E) and examined under a light microscope by an independent pathologist blinded to the treatment modes.

### **Data Analysis**

Contrast volume and intensity were analyzed using OsiriXVP software on a Mac OS platform. Contrast volumes were outlined on each T1 contrast slice and calculated according to the following equation:  $V = (S_i \times 0.15) \text{ cm}^3$  where  $S_i$  represents the contrast area calculated on each 1.5 mm thick slice.

## **Results**

### **Local PDT-Induced BBB Disruption**

Localized regions of increased signal intensity on T1-weighted MRI scans were used as a marker of BBB disruption in the rat brain. Both the volume of the enhancing region and the signal intensity were measured at a specific time interval following i.p. contrast injection. Four

to five hours following ALA injection (125 mg/kg i.p.) light treatment was given to three groups of rats ( $n = 6$  per group) to a fluence level of 9, 17 or 26J using a fluence rate of 10 mW. Figure 2a,b illustrate typical post-contrast MRI scans performed 3–4 hours after PDT treatment. A fluence level of either 9 or 17 J was used and the scans taken 15 minutes following i.p. contrast injection. Clear evidence of local BBB disruption is seen at both fluence levels as evidenced by the localized contrast enhancement (Fig. 2a,b) centered around the stereotactic placement position of the light delivery fiber tip.

Figure 3 shows the average volume of contrast enhancement measured from MRI scans performed post-treatment for the three light fluences. A significant light dose response effect was apparent, with increasing light fluence giving increased contrast volume indicating an increasing disruption of the BBB. Similar results were seen for enhancement intensity as shown in Figure 4a. The concentration of the contrast medium (calculated from the calibration curve in Fig. 1) is shown in Figure 4b. Contrast concentrations between 125 and 710  $\mu\text{g/ml}$  were obtained for the three fluence levels examined (9–26 J). In the absence of ALA (light-only control), high fluences (26 J) demonstrated no apparent increased signal level in the region of light treatment compared to normal brain.

In a separate set of experiments designed to evaluate fluence rate effects, rats were treated to a total fluence of 26 J delivered at 10, 30, or 50 mW. The effects of fluence rate on contrast volume are shown in Figure 5. Increased fluence rates gave not only increased contrast volume but increased signal intensity as well, indicating an increased contrast concentration.

### Time Course of BBB Opening and Closing

One group of four animals was subjected to a fluence of 9 J while another four rats were treated to a fluence level of 17 J. In both cases, light was delivered at a fluence rate of 10 mW. The animals were scanned 2–4 hours following treatment and rescanned 1, 3, 7, and 17 days post-treatment. The animals were scanned 15 minutes following i.p. contrast injection. Figure 6 shows the T1 contrast images from one of the animals in each group scanned shortly after PDT and 24 and 72 hours following light treatment. A localized contrast enhancement is clearly seen 2–4 hours following light treatment at both fluence levels. For a fluence of 9 J, the BBB was restored by day 3 (Fig. 6c). For higher fluence levels (17 or 26 J), the BBB disruption lasted for a longer duration and, in some cases, was still not completely restored by day 17. Figure 7 illustrates the increase of T1 signal intensity with time post-contrast injection on day 1 and 7 following light treatment. The signal intensity 24 hours following PDT treatment and 60 minutes post-contrast injection was considered as the 100% point. The rate of flow was clearly biphasic on day 1 with a rapid increase in intensity during the initial 10 minutes following contrast injection and thereafter decreasing to a much lower rate following the initial contrast influx. Interestingly, a linear increase in average intensity with time was observed on all subsequent scanning days in all the animals tested.

Contrast flow rate, based on increasing volume of T1 signal enhancement, on each of these days was calculated by rescanning the rats at several intervals following contrast injection. The combined average results for a fluence level of 17 J for all four animals are shown in Figure 8. The rate of flow fell rapidly from 7 to 1.3  $\mu\text{l/minutes}$  (80% decrease) from day 0–1 to day 3. Thereafter, the flow rate decreased at a decreasing rate and approximated base line flow after 17 days.

### Histological Analysis

In areas exposed to the highest fluence levels (5–15  $\mu\text{m}$  from the fiber), no significant pathology was observed in coronal sections obtained from animals subjected to fluences of 9 J (Fig. 2c). At higher fluence levels of 17 J, extensive infiltration of lymphocytes and macrophages (some

loaded with hemosiderin) was apparent (Fig. 2d). Blood vessels in these sections showed hyperplastic endothelial cells. At fluence levels of 26 J, a focally extensive area of necrosis with some degeneration of brain parenchyma and infiltration of lymphocytes, plasma cells and foamy macrophages (Gitter cells), was apparent in the immediate area of the fiber tip. Some of the Gitter cells contained hemosiderin which is suggestive of treatment-induced hemorrhage. Blood vessels in these sections also showed hyperplastic endothelium. In contrast, sections taken 1, 2 or 3 mm from the fiber track showed no significant pathology for all three of the fluence levels tested.

Histological sections taken from the brains of light-only control animals showed no pathology.

## Discussion

Malignant gliomas are characterized by a large central volume of extensive necrosis surrounded by a shell of viable tumor cells. In magnetic resonance images, the tumor appears with a clearly delineated boundary, however, histological examination invariably shows a zone of infiltrated brain. Invading tumor cells may be chemo-resistant by virtue of their location in areas of the brain where the BBB is intact, and their tendency to reside in the non-proliferative  $G_0$  phase of the cell cycle [16].

The limited access of therapeutic agents into tumor infiltrated brain resulting from the presence of the BBB emphasizes the need for developing strategies for bypassing the BBB. The BBB is a specialized vascular system consisting of endothelial cells with highly selective membranes connected by tight junctions. Molecular size, charge and lipid solubility are the primary factors that limit passage of drugs through the BBB. Attempts to develop pharmaceuticals capable of circumventing the BBB, such as lipid-soluble or water-soluble drugs with high affinities for natural carriers [17,18] have proven only partially successful. Intra-arterial infusion of mannitol, which causes dehydration and shrinkage of endothelial cells, results in opening of the tight junctions and a non-localized BBB disruption. This widespread opening of the BBB results in unwanted side effects since potent cytotoxic drugs gain access to both the tumor as well as normal brain in equal quantities. Treatment-related toxicity [19] as well as a number of technical difficulties associated with intra-arterial drug delivery, have prevented the widespread use of this technique.

Localized methods of drug delivery that bypass the BBB altogether, such as direct intratumoral injection [20,21] convection-enhanced delivery [22–24] and controlled release from polymer implants [25,26] can carry an increased risk of morbidity and mortality and have only shown a modest benefit. Focused ultrasound offers a method to disrupt the BBB non-invasively and reversibly at targeted locations [27,28]. This technique though is not well suited to the complex geometry or size of a postoperative resection cavity.

In this study we have shown that the commonly used MRI contrast agent Gd-DTPA (molecular weight: 938), was clearly evident in a localized region in the immediate vicinity of the illuminating fiber. Since Gd-DTPA does not pass the intact BBB, leakage of this contrast agent, and the resulting increased signal intensity on MRI scans, was used as a surrogate for a putative anti-cancer agent. In a recent study using ultrasound to open the BBB, Treat et al. [28] found a strong correlation between MRI signal intensity and the concentration of Doxorubicin in the targeted regions of the brain. These findings indicate that contrast enhanced MRI is a useful non-invasive tool in predicting the degree of penetration of chemotherapy agents through the disrupted BBB.

The volume and concentration of contrast was found to be light dose dependent (Figs. 3 and 4). PDT at increasing fluence levels between 9 and 26 J demonstrated an increasing contrast flow rate. This suggests the possibility of adjusting the drug penetration into the tissue. This

has to be balanced with the observation that fluences over 9 J resulted in a certain amount of local tissue damage which suggests an upper limit to the maximum fluence that can be employed. In addition, fluence rates over 10 mW induced pronounced brain edema which often led to increased morbidity and even death.

No effect on the BBB was observed if 26 J of light was given in the absence of ALA. This indicates that neither the direct trauma of fiber insertion, or thermal effects caused by light energy absorption, played a significant role in BBB disruption.

The degradation of the BBB was temporary in nature, opening rapidly following treatment and significantly restored during the ensuing 72 hours. The BBB was found to be disrupted as early as 2 hours following PDT and approximately 90% restored 72 hours later. From a therapeutic standpoint, this time window is sufficient for the application of anti-cancer agents.

The mechanisms by which PDT leads to BBB degradation are uncertain but they likely include direct PDT effects on the endothelial cytoskeleton that lead to cell rounding and contraction, probably mediated by PDT-induced microtubule depolarization [29]. In addition the formation and/or enlargement of endothelial gaps, has been observed in response to PDT [30].

In previous fluorescence microscopy studies [5], ALA-induced protoporphyrin IX (PpIX) fluorescence dropped sharply at the tumor/brain border. Even so, some PpIX fluorescence was apparent in presumptive normal brain in close proximity to the boundary. For example, at 1 and 2 mm from the tumor/brain boundary, the fluorescence was 13% and 2.5% of that observed in bulk tumor, respectively. This indicates that a direct effect on the capillary endothelial cells is the most probable cause for the BBB degradation.

Low fluence rate/low fluence PDT has been demonstrated to enhance the delivery of macromolecular drug carriers, in particular liposomally encapsulated doxorubicin (Doxil) into murine colon carcinoma tumors growing in the shoulders of mice [31]. We have also observed a significant increase in edema formation, in orthotopic brain tumors, following ALA-mediated PDT in a rat brain tumor model indicating a breakdown of the blood–tumor barrier (BTB) [5, 14]. In these cases, the BTB was significantly altered by PDT most probably in a similar manner to the one proposed here for the BBB by enlarging endothelial gaps. In a recent article, Hu et al. [32], using a rat C6 glioma model and electron microscopy, showed that PDT changed the sub-cellular structure of the BTB with a reduction in the number of cellular components in endothelial cells of the capillary blood vessels. They also observed stretching of the tight junctions, with an enlargement of the gaps between endothelial cells and. In addition, PDT was found to have only a minimal impact on the normal sub-cellular structures of the BBB suggesting that the endothelial cells comprising the BBB were not permanently damaged by the treatment. These observations are in good agreement with the findings of this study which showed that low fluence PDT was capable of inducing BBB disruption, as evidenced by contrast enhancement on MR images, yet no permanent damage was found in histological sections (Fig. 2). In contrast, the results of the present study clearly show that high fluence levels are capable of causing significant tissue damage. For example, the tissue damage and immune cell infiltration observed in the region in close proximity to the light source are consistent with cerebral ischemia resulting in a localized stroke. Contrast enhancement following Gd–DTPA injection is considered to be one of the signatures of BBB breakdown in cerebral ischemia. The region of tissue damage was limited in extent, and sections 1 mm from the point of maximum light intensity were unaffected. In a clinical setting, with light delivered directly into the wall of the tumor resection cavity, a much lower fluence rate would be applied to the surrounding brain. PDT could therefore offer an alternative to other strategies that have been developed to circumvent the BBB. For a drug delivery system to be successful, transient,

and localized targeting of BBB disruption is necessary. PDT applied through an indwelling balloon applicator filling the resection cavity, could meet this requirement [33].

In this study we have demonstrated that ALA-mediated PDT causes disruption of the BBB in a fluence and fluence rate dependent manner. At low fluence levels, the duration of BBB opening was less than 72 hours following treatment. No permanent tissue damage was observed in this case. Although the degree of BBB disruption was greater at higher fluence levels, damage to the surrounding tissue was evident. Localized T1-weighted MRI signal intensity observed following contrast injection proved to be a highly effective and non-invasive modality for following the development of the degree and time course of BBB dysfunction thus allowing the use of fewer animals.

## Acknowledgements

Henry Hirschberg is grateful for the support of the Norwegian Radiumhospital Research Foundation. Steen Madsen is grateful for the support of the UNLV Office of Research. Portions of this work were made possible, in part, through access to the Laser Microbeam and Medical Program (LAMMP) and the Chao Cancer Center Optical Biology Shared Resource at the University of California, Irvine. These facilities are supported by the National Institutes of Health under grants RR-01192 and CA-62203, respectively. In addition, Beckman Laser Institute programmatic support was provided by the Department of Energy (DOE #DE-FG03-91ER61227), and the Office of Naval Research (ONR #N00014-91-C-0134).

Contract grant sponsor: Norwegian Radium Hospital Research Foundation; Contract grant sponsor: UNLV Office of Research; Contract grant sponsor: Laser Microbeam and Medical Program (LAMMP); Contract grant sponsor: Chao Cancer Center Optical Biology Shared Resource at the University of California, Irvine; Contract grant sponsor: National Institutes of Health; Contract grant numbers: RR-01192, CA-62203; Contract grant sponsor: Beckman Laser Institute; Contract grant numbers: DOE #DE-FG03-91ER61227, ONR #N00014-91-C-0134.

## References

1. Wallner KE, Galicich JH, Krol G, Arbit E, Malkin MG. Patterns of failure following treatment for glioblastoma multiforme and anaplastic astrocytoma. *Int J Radiat Oncol Biol Phys* 1989;16:1405–1409. [PubMed: 2542195]
2. Kroll RA, Neuwelt EA. Outwitting the blood-brain barrier for therapeutic purposes: Osmotic opening and other means. *Neurosurgery* 1998;42:1083–1099. [PubMed: 9588554]
3. Siegal T, Zylber-Katz E. Strategies for increasing drug delivery to the brain. *Clin Pharmacokinet* 2002;41:171–186. [PubMed: 11929318]
4. Groothuis DR, Fischer JM, Vick NA, Bigner DD. Comparative permeability of different glioma models to horseradish peroxidase. *Cancer Treat Rep* 1981;65:13–18. [PubMed: 6179614]
5. Angell-Petersen E, Madsen SJ, Spetalen S, Sun CH, Peng Q, Carper SW, Hirschberg H. Influence of light fluence rate on the effects of photodynamic therapy in an orthotopic rat glioma model. *J Neurosurg* 2006;104(1):109–117. [PubMed: 16509154]
6. Dougherty TJ, Gomer CJ, Henderson BW, Jori G, Kessel D, Korbelik M, Moan J, Peng Q. Review: Photodynamic therapy. *J Nat Can Inst* 1998;90:889–905.
7. Cheng MS, McKean J, Boisvert D. Photoradiation therapy: Current status applications in the treatment of brain tumours. *Surg Neurol* 1986;25:423–435. [PubMed: 2938288]
8. Muller PJ, Wilson BC, Lilge LD, Yang V, Hetzel FW, Chen Q, Selker R, Abrams J. Photofrin photodynamic therapy for malignant brain tumors. *Proc SPIE* 2001;4248:34–41.
9. Eljamel MS, Goodman C, Moseley H. ALA and Photofrin® Fluorescence-guided resection and repetitive PDT in glioblastoma multiforme: A single centre Phase III randomized controlled trial. *Lasers Med Sci*. 2007 Oct 10; epub ahead of print
10. Madsen SJ, Sun CH, Tromberg BJ, Hirschberg H. Repetitive ALA-mediated photodynamic therapy on human glioma spheroids. *J Neurooncol* 2003;62:243–250. [PubMed: 12777075]
11. Hirschberg H, Angell-Petersen E, Peng Q, Tromberg B, Sun CH, Madsen SJ. Repetitive photodynamic therapy of malignant brain tumors. *J Environ Pathol Toxicol Oncol* 2006;25(1–2): 261–280. [PubMed: 16566723]

12. Stummer W, Goetz C, Hassan A, Heimann DVM, Kempfski O. Kinetics of Photofrin II in perifocal brain edema. *Neurosurgery* 1993;33:1075–1082. [PubMed: 8133993]
13. Hebeda KM, Saarnak AE, Olivo M. 5-Aminolevulinic acid induced endogenous porphyrin fluorescence in 9L and C6 brain tumours and in the normal rat brain. *Acta Neurochir* 1998;140:503–513.
14. Hirschberg H, Mathews MS, Angell-Petersen E, Spetalen S, Madsen SJ. Increased brain edema following 5-aminolevulinic acid administration mediated photodynamic therapy in normal and tumor-bearing rats. *Proc SPIE* 2007;6424:64242B1–64242B8.
15. Itoi S, Rachinger W, Stepp H, Reulen HJ, Stummer W. Oedema formation in experimental photoradiation therapy of brain tumours using 5-ALA. *Acta Neurochir (Wien)* 2005;147:57–65. [PubMed: 15565479]
16. Giese A, Loo MA, Tran N, Haskett D, Coons SW, Berens ME. Dichotomy of astrocytoma migration and proliferation. *Int J Cancer* 1996;67:275–282. [PubMed: 8760599]
17. Jolliet-Riant P, Tillementi JP. Drug transfer across the blood–brain barrier and improvement of brain delivery. *Fund Clin Pharmacol* 1999;13:16–26.
18. Pardridge WM. Blood-brain barrier drug targeting: The future of brain drug development. *Mol Interv* 2003;3(2):90–105. [PubMed: 14993430]
19. Doolittle ND, Miner ME, Hall WA, Siegal T, Jerome E, Osztie E, McAllister LD, Bubalo JS, Kraemer DF, Fortin D, Nixon R, Muldoon LL, Neuwelt EA. Safety and efficacy of a multi-center study using intra-arterial chemotherapy in conjunction with osmotic opening of the blood-brain barrier for the treatment of patients with malignant brain tumors. *Cancer* 2000;88(3):637–647. [PubMed: 10649259]
20. Rand RW, Kreitman RJ, Patronas N, Varricchio F, Pastan I, Puri RK. Intratumoral administration of recombinant circularly permuted interleukin-4-Pseudomonas exotoxin in patients with high-grade glioma. *Clin Cancer Res* 2000;6(6):2157–2165. [PubMed: 10873064]
21. Sampson JH, Akabani G, Archer GE, Bigner DD, Berger MS, Friedman AH, Friedman HS, Herndon JE, Kunwar S, Marcus S, McLendon RE, Paolino A, Penne K, Provenzale J, Quinn J, Reardon DA, Rich J, Stenzel T, Tourt-Uhlig S, Wikstrand C, Wong T, Williams R, Yuan F, Zalutsky MR, Pastan I. Progress report of a Phase I study of the intra-cerebral microinfusion of a recombinant chimeric protein composed of transforming growth factor (TGF)-alpha and a mutated form of the Pseudomonas exotoxin termed PE-38 (TP-38) for the treatment of malignant brain tumors. *J Neurooncol* 2003;65(1):27–35. [PubMed: 14649883]
22. Bobo RH, Laske DW, Akbasak A, Morrison PF, Dedrick RL, Oldfield EH. Convection-enhanced delivery of macromolecules in the brain. *Proc Natl Acad Sci* 1994;91:2076–2080. [PubMed: 8134351]
23. Lieberman DM, Laske DW, Morrison PF, Bankiewicz KS, Oldfield EH. Convection-enhanced distribution of large molecules in gray matter during interstitial drug infusion. *J Neurosurg* 1995;82:1021–1029. [PubMed: 7539062]
24. Lidar Z, Mardor Y, Jonas T, Pfeffer R, Faibel M, Hadani M, Ram Z. Convection-enhanced delivery of paclitaxel for the treatment of recurrent glioblastoma. A phase I/II clinical study. *J Neurosurg* 2004;100:472–479. [PubMed: 15035283]
25. Brem H, Piantadosi S, Burger PC, Walker M, Selker R, Vick NA, Black KL, Sisti M, Brem S, Mohr G, Muller P, Morawetz R, Schold SC. For the Polymer-Brain Tumor Treatment Group: Placebo-controlled trial of safety and efficacy of intraoperative controlled delivery by biodegradable polymers of chemotherapy for recurrent gliomas. *Lancet* 1995;345(8956):1008–1012. [PubMed: 7723496]
26. Lawson HC, Sampath P, Bohan E, Park MC, Hussain N, Olivi A, Weingart J, Kleinberg L, Brem H. Interstitial chemotherapy for malignant gliomas: The Johns Hopkins experience. *J Neurooncol* 2007;83(1):61–70. [PubMed: 17171441]
27. Choi JJ, Pernot M, Small SA, Konofagou EE. Noninvasive, transcranial and localized opening of the blood-brain barrier using focused ultrasound in mice. *Ultrasound Med Biol* 2007;33(1):95–104. [PubMed: 17189051]
28. Treat LH, McDannold N, Vykhodtseva N, Zhang Y, Tam K, Hynynen K. Targeted delivery of doxorubicin to the rat brain at therapeutic levels using MRI-guided focused ultrasound. *Int J Cancer* 2007;121:901–907. [PubMed: 17437269]



29. Sporn LA, Foster TH. Photofrin and light induces microtubule depolymerization in cultured human endothelial cells. *Cancer Res* 1992;52:3443–3448. [PubMed: 1534512]
30. Fingar VH. Vascular effects of photodynamic therapy. *J Clin Laser Med Surg* 1996;14:323–328. [PubMed: 9612199]
31. Snyder JW, Greco WR, Bellnier DA, Vaughan L, Henderson BW. Photodynamic therapy: A means to enhanced drug delivery to tumors. *Cancer Res* 2003;63:8126–8131. [PubMed: 14678965]
32. Hu SS, Cheng HB, Zheng YR, Zhang RY, Yue W, Zhang H. Effects of photodynamic therapy on the ultrastructure of glioma cells. *Biomed Environ Sci* 2007;20(4):269–273. [PubMed: 17948759]
33. Madsen SJ, Sun CH, Tromberg BJ, Hirschberg H. Development of a novel balloon applicator for optimizing light delivery in photodynamic therapy. *Lasers Surg Med* 2001;29:406–412. [PubMed: 11891728]

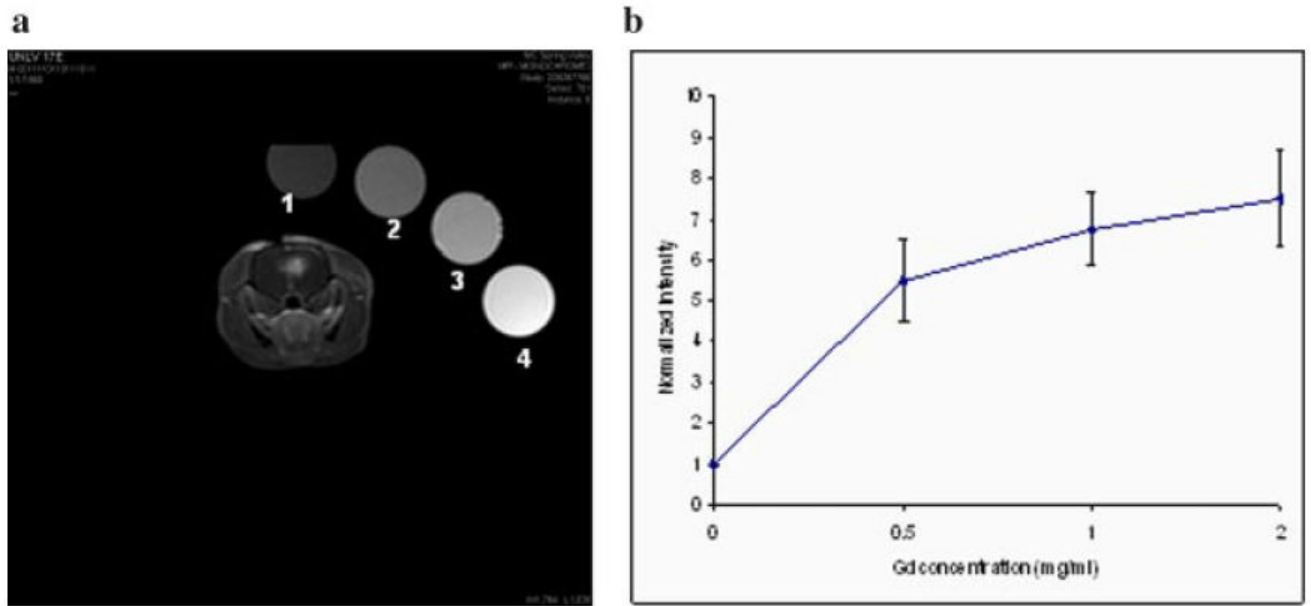


**Fig. 1.**  
**a:** T1-weighted MR images of a PDT-treated rat along with four calibration tubes with Gd concentrations of 0, 0.5, 1, and 2 mg/ml. **b:** Normalized signal intensity as a function of Gd concentration.

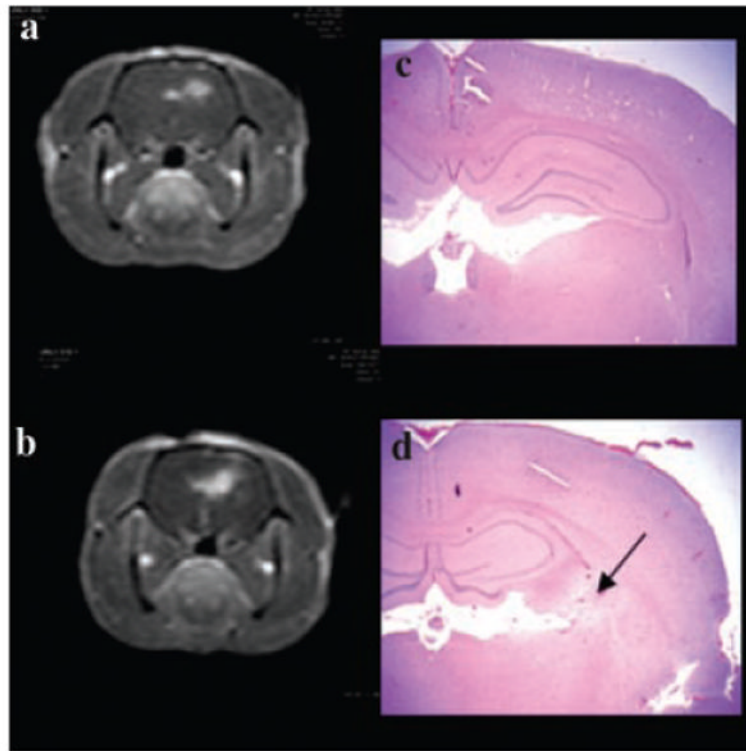


**Fig. 2.** T1-weighted MRI contrast enhanced images (**a, b**) showing focal contrast enhancement centered around the area of light treatment. PDT treatment to a fluence level of 9 (a) and 17 J (b), at a fluence rate of 10 mW was performed 4 hours following ALA administration (125 mg/kg i.p.). Both scans were performed 3–4 hours post-PDT and 15 minutes following i.p. contrast injection. (**c, d**) Coronal H&E sections from the brains of animals corresponding to a and b taken 14 days post-treatment. In the area exposed to the highest fluence level (5–15  $\mu\text{m}$  from the fiber) no significant pathology was observed following delivery of 9 J (c). At a fluence level of 17 J, extensive infiltration of lymphocytes and macrophages (some loaded with hemosiderin) was apparent as denoted by the arrow in (d).

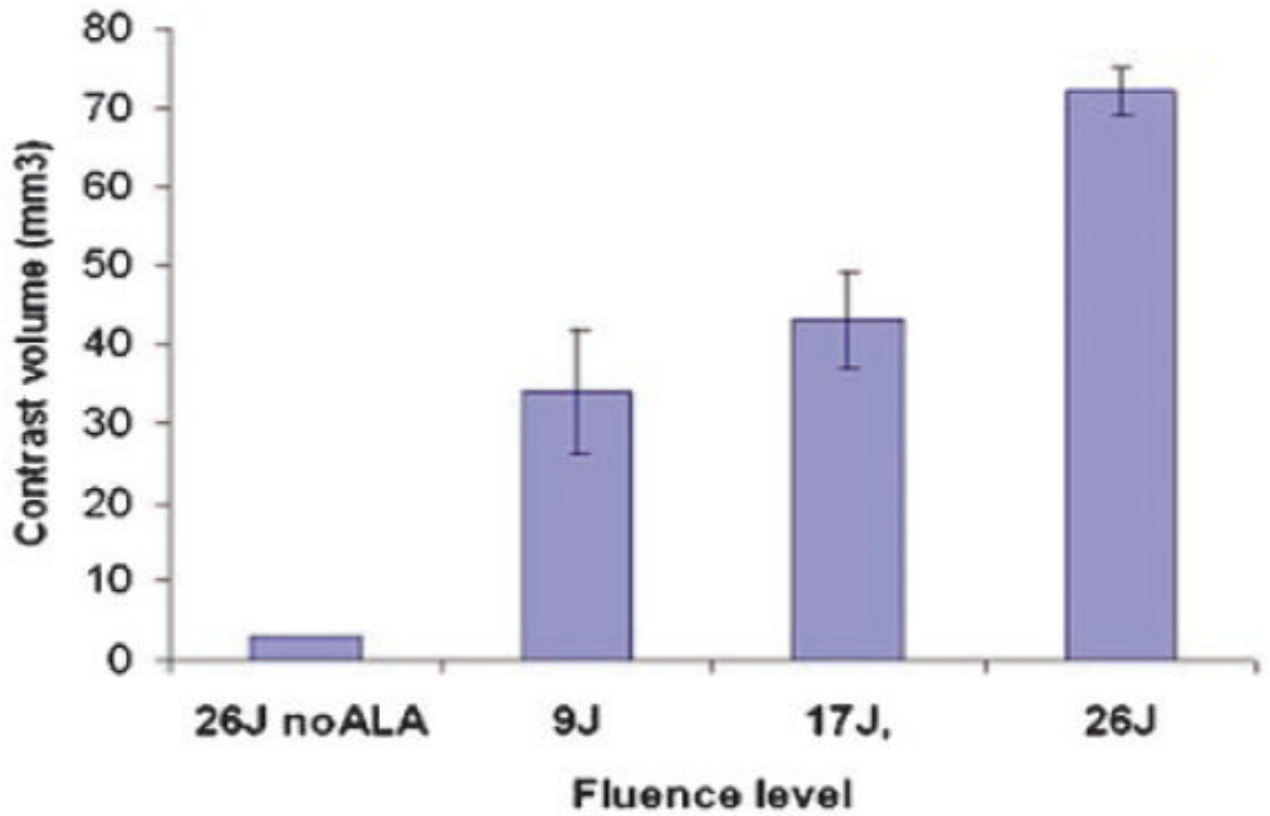


**Fig. 3.**

Average contrast volume measured from MRI scans performed 24 hours post-treatment for three light fluences (fluence rate = 10 mW). A significant light dose response was apparent, with increasing light fluence resulting in increased contrast. A fluence of 26 J, in the absence of ALA (light-only control), resulted in minimal contrast enhancement suggesting an intact BBB.

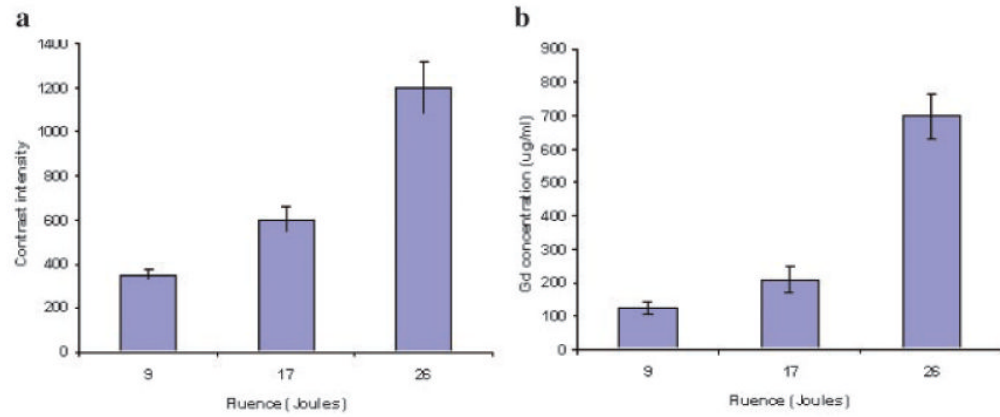


**Fig. 4.**

**a:** Average contrast intensity measured from T1-weighted MR images performed 24 hours post-treatment for three light fluences. Images were obtained 15 minutes post-contrast injection.

**b:** Concentration of contrast medium calculated from the calibration curve shown in Figure 1. Contrast concentrations between 125 and 710 µg/ml were obtained for the three fluence levels examined.

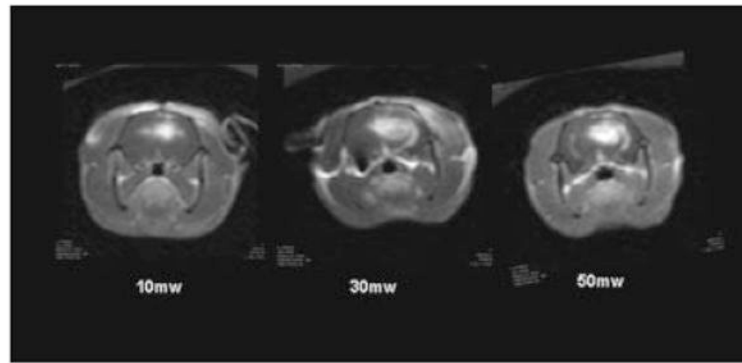


**Fig. 5.** T1-weighted MRI contrast enhanced images showing focal contrast enhancement as evidence of BBB disruption. The effects of fluence rate on BBB disruption are clearly evident. Increased fluence rates resulted not only in increased contrast volume but increased signal intensity as well, indicating an increased contrast concentration.

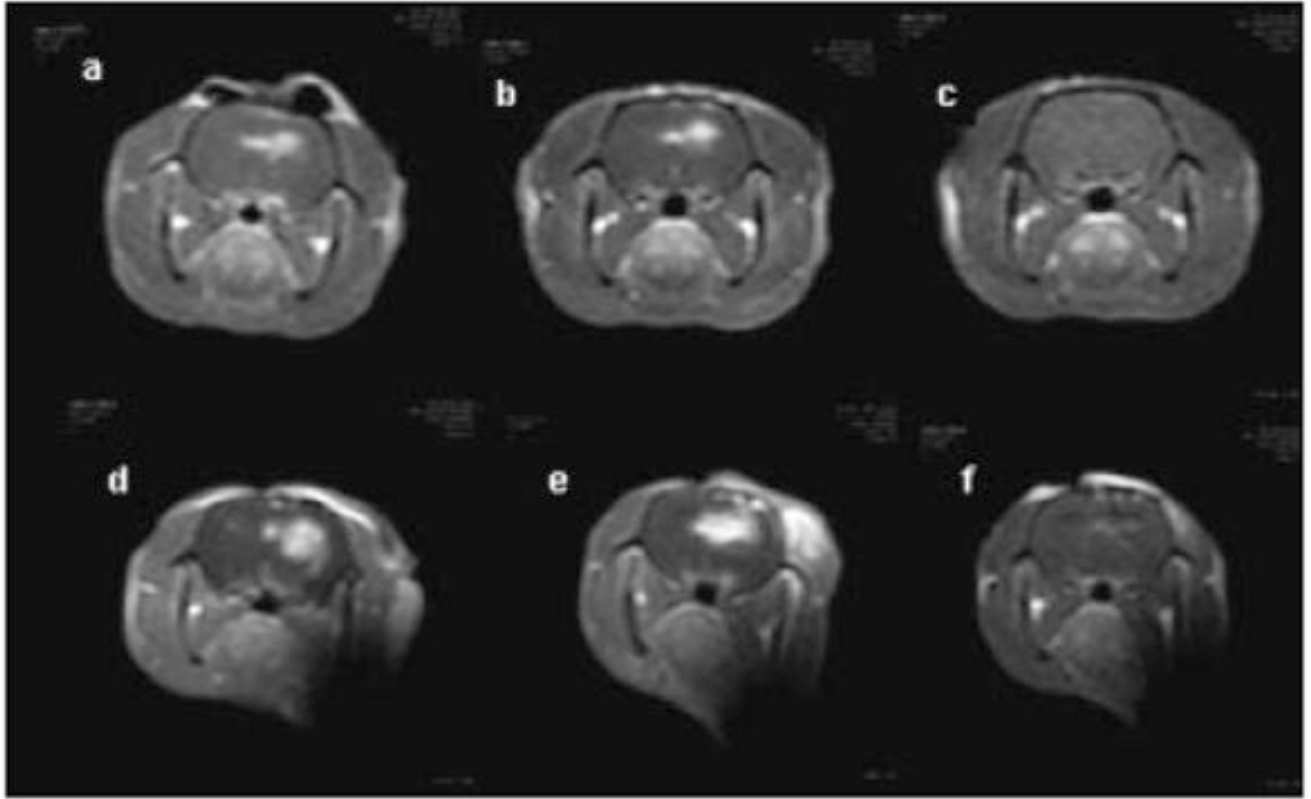


**Fig. 6.** T1-weighted MRI contrast enhanced images showing focal contrast enhancement at 2 (a), 24 (b) and 72 (c) hours post-treatment, respectively. PDT treatments using 9 J (a,b,c) or 17 J (d,e,f) were performed at a fluence rate of 10 mW. All animals were scanned 15 minutes, following i.p. contrast injection. A localized contrast enhancement is clearly seen 2 and 24 hours following light treatment (a,b,d,e) for both 9 and 17 J. Images taken 72 hours following treatment with 9 J showed no enhancing regions (c) while reduced enhancement persisted up to day 7 following PDT with 17 J (f).

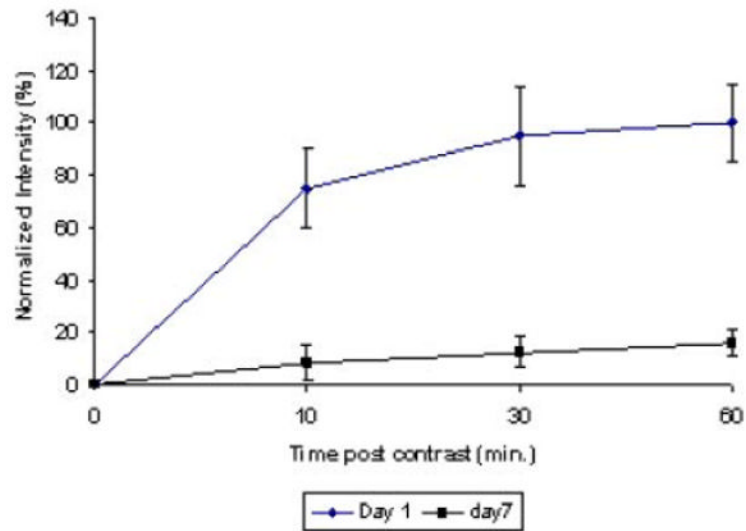


**Fig. 7.**

T1 signal intensity with time post-contrast injection on days 1 and 7 following light treatment. The signal intensity 24 hours following PDT treatment and 60 minutes post-contrast injection was considered as the 100% point. The rate of flow was clearly biphasic on day 1 with a rapid increase in volume during the initial 10 minutes, following contrast injection and decreasing to a much lower rate following the initial contrast influx. A greatly reduced and linear increase in average intensity with time was observed on day 7.



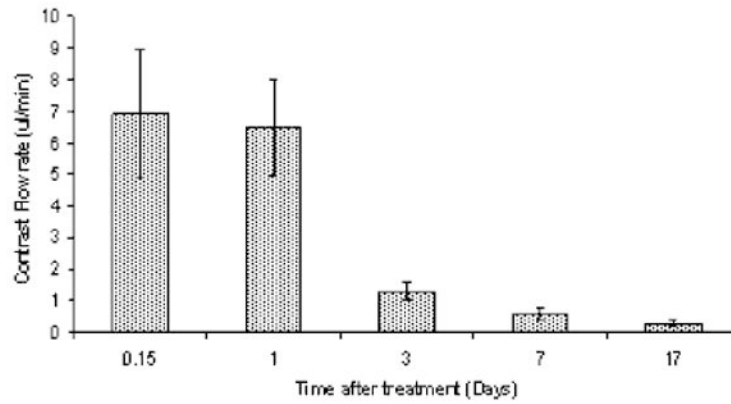


**Fig. 8.** Time course of BBB closing. Scanning was performed 4 hours and 1,3,7, and 17 days post-PDT treatment to determine changes in the BBB with time. Contrast flow rate, based on increasing volume of T1 signal intensity, on each of these days was calculated by rescanning the rats at several intervals following contrast injection. The rate of flow fell rapidly from 6.7 to 1.3  $\mu\text{l}/\text{minutes}$  (80% decrease) from day 1 to day 3. PDT treatment was performed 4 hours following i.p. injection of 125 mg/kg ALA. All animals were subjected to light fluence and fluence rates of 17 J and 10 mW, respectively.